Supplemental Table 1. Human PK predictions for JNJ311.

	Mouse[†]	Rat[†]	Dog[†]	Human
Unbound plasma fraction (%)	36.8	36.9	36.9	37.1
Dose JNJ311 (mg/kg)[*]	0.25	0.25	0.25	0.25 (pred.)
Plasma clearance (mL/min/kg)	193 ± 63	116 ± 10	77 ± 16	1.05[‡], 1.285[§]
Liver blood flow (%)	> 100	> 100	> 100	-
Volume of distribution at steady state (L/kg)	4.0 ± 0.7	4.5 ± 0.9	4.0 ± 1.0	2.98[‡], 3.96[§]
Elimination half-life (h)	0.3 ± < 0.1	0.4 ± 0.1	0.7 ± 0.1	0.7[‡] , 2.4[§]
*Formulations with 20% HPβCD aq, [†]values represent mean ± standard deviation from 3 animals, [‡]predicted value using Dedrick approach, [§]predicted value using allometric scaling				

Supplemental Table 2. Biodistribution of ^{18}F-JNJ311 and ^{18}F-AV1451 in NMRI mice at 2, 10, 30 and 60 min p.i.*

Body part	^{18}F-JNJ311				^{18}F-AV1451			
	2 min	10 min	30 min	60 min	2 min	10 min	30 min	60 min
Blood	0.5 ± 0.1	0.3 ± 0.1	0.2 ± 0.0	0.1 ± 0.0	0.4 ± 0.1	0.3 ± 0.0	0.2 ± 0.0	0.2 ± 0.0
Bone	0.5 ± 0.2	0.7 ± 0.1	0.6 ± 0.1	0.5 ± 0.1	0.6 ± 0.4	0.5 ± 0.1	0.7 ± 0.1	0.9 ± 0.2
Brain	1.9 ± 0.1	0.8 ± 0.2	0.3 ± 0.0	0.1 ± 0.0	2.2 ± 0.3	1.0 ± 0.2	0.2 ± 0.1	0.1 ± 0.0
Cerebellum	1.9 ± 0.2	0.7 ± 0.1	0.2 ± 0.1	0.1 ± 0.0	2.4 ± 0.5	0.9 ± 0.2	0.2 ± 0.1	0.1 ± 0.0
Cerebrum	1.9 ± 0.1	0.8 ± 0.1	0.3 ± 0.1	0.1 ± 0.0	2.1 ± 0.3	1.0 ± 0.2	0.3 ± 0.1	0.1 ± 0.0
Heart	2.3 ± 0.8	1.1 ± 0.6	0.4 ± 0.1	0.1 ± 0.1	2.0 ± 0.4	0.8 ± 0.1	0.4 ± 0.1	0.3 ± 0.0
Kidneys	10.6 ± 2.9	8.1 ± 2.5	2.9 ± 0.6	0.9 ± 0.1	10.4 ± 2.4	9.7 ± 1.0	4.9 ± 1.5	3.8 ± 0.7
Liver	2.6 ± 0.6	4.6 ± 0.7	3.4 ± 0.4	1.6 ± 0.3	3.6 ± 0.6	5.6 ± 0.5	6.5 ± 0.6	5.3 ± 0.6
Lungs	8.3 ± 4.6	2.6 ± 1.3	1.0 ± 0.3	0.2 ± 0.1	7.0 ± 2.5	1.6 ± 0.6	1.2 ± 0.3	0.6 ± 0.2
Muscle	1.4 ± 0.1	0.6 ± 0.0	0.2 ± 0.1	0.1 ± 0.0	0.9 ± 0.5	0.5 ± 0.1	0.2 ± 0.0	0.1 ± 0.0
Pancreas	1.4 ± 0.4	1.8 ± 0.4	0.8 ± 0.1	0.2 ± 0.0	1.2 ± 0.6	1.8 ± 0.3	0.7 ± 0.3	0.4 ± 0.1
Spleen	4.9 ± 0.7	2.3 ± 1.0	0.8 ± 0.2	0.2 ± 0.0	4.5 ± 1.6	5.2 ± 4.8	1.2 ± 0.4	0.9 ± 0.4
	2/60 min				2/60 min			
Brain	29.6				18.3			
Blood	7.5				2.4			

*Data are expressed as SUV mean ± standard deviation; n = 3 per time point; ratios were calculated using non rounded values

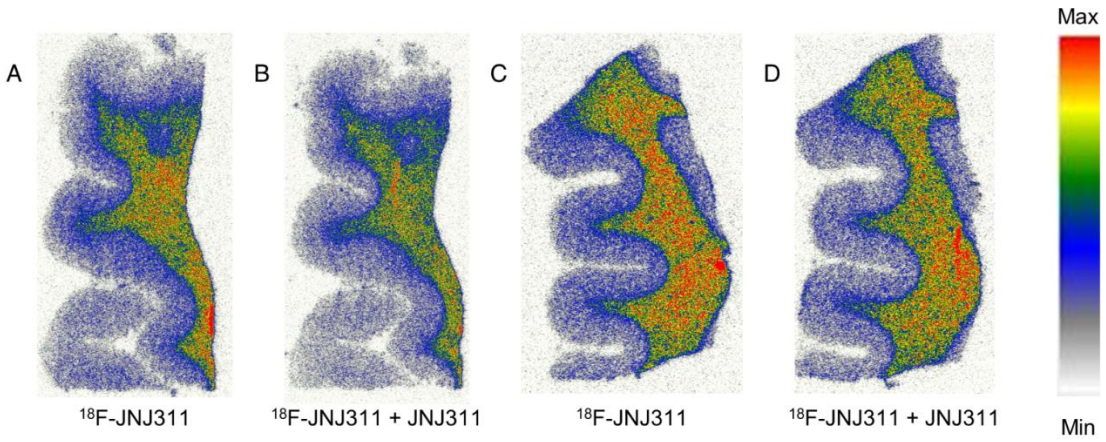

Supplemental Figure 1. Adjacent, 10-µm-thick, post-mortem human PSP (A and B) and CBD (C and D) brain slices of the frontal cortex of a PSP patient (71-year-old) and CBD patient (74-year-old) incubated with ^{18}F-JNJ311 (740 kBq / 500 µL / slice) (A and C) in the presence of authentic reference compound JNJ311 (B and D) at 1 µmol/L.

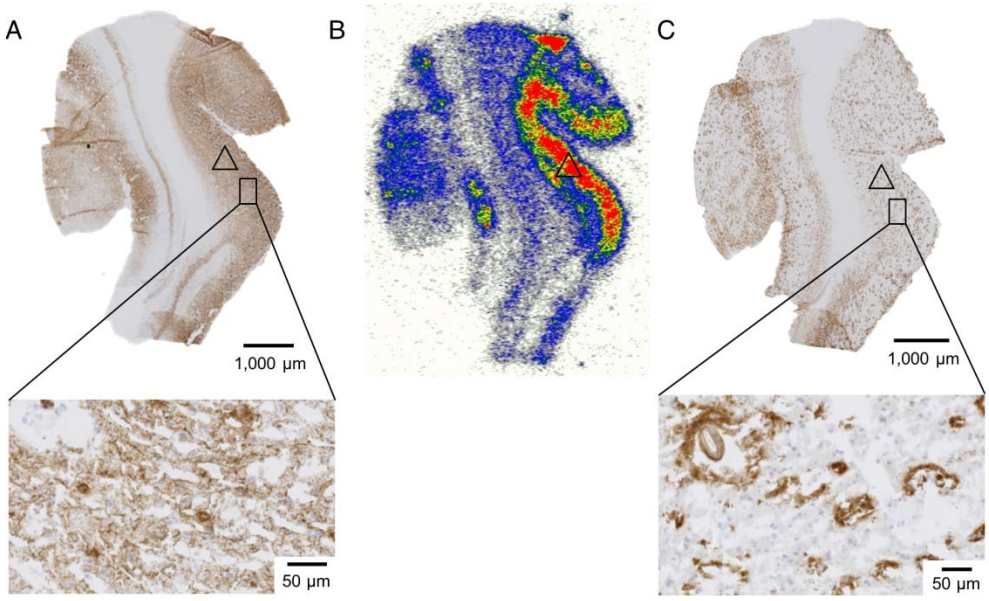

Supplemental Figure 2. Autoradiographic analysis on 10-µm-thick slices of the visual cortex of an AD patient (68-year-old with Braak stage VI) with ^{18}F-JNJ311 (B). Adjacent slices were immunostained for tau (A, AT8, 1000-µm scale bar) and for β-amyloid (C, 4G8, 1000-µm scale bar). Higher magnification at the bottom identifies tau pathology (50-µm scale bar) and β-amyloid plaques (50-µm scale bar). Triangle indicates area of high density of PHF deposits and relatively low density of β-amyloid deposits.

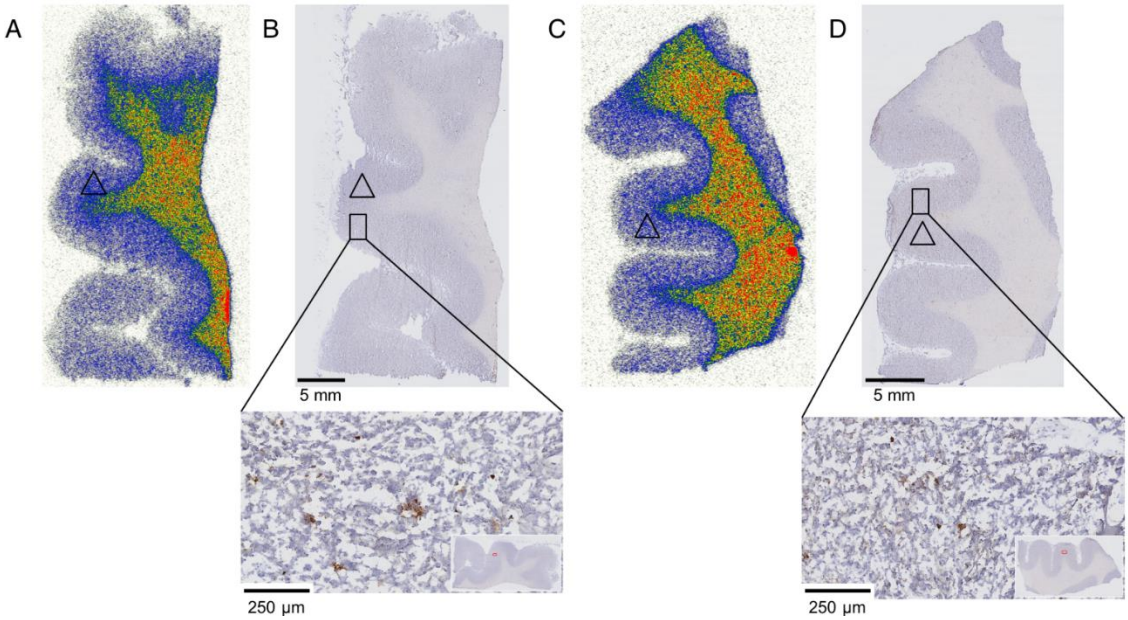

Supplemental Figure 3. Autoradiographic analysis on 10-µm-thick slices of the frontal cortex of a PSP patient (71-year-old; A and B) and CBD patient (74-year-old; C and D) with ^{18}F-JNJ311 (A and C). Adjacent slices were immunostained for tau (B and D, AT8, 5-mm scale bar). Higher magnification at the bottom identifies tau pathology (250-µm scale bar). Triangle indicates area of medium density of hyperphosphorylated tau deposits.

Supplemental Table 3. pIC_{50}/K_i (nM) values for purified tau and β-amyloid and molecular features of all compounds.*

Compound	pIC_{50} – tau	K_i – tau	pIC_{50} - Aβ	K_i - Aβ	PSA (Å²)‡	$LogD_{7.4}$†
JNJ311	7.7	8	< 5	> 4398	51	2.2
AV1451	8.4	1	6.2	278	42	2.2
AV680	7.7	7	5.0	4934	33	3.0
AV45	5.2	> 2323	7.6	12	53	3.1

*pIC_{50} values were determined from displacement curves of 2-5 independent experiments, K_i values were calculated from IC_{50} values using the following equation: $K_i = IC_{50}/(1+$ (concentration RL/ K_D RL), with a K_D for PHF of 6.275 nM for ^{3}H-AV680, a K_D for β-amyloid of 7.85 nM for ^{3}H-AV45, and 10 nM of RL concentration in both assays; †$LogD_{7.4}$ value was chromatographically determined for JNJ311, but calculated for the other compounds; ‡PSA = polar surface area

Supplemental Table 4. Relative percentages of intact tracer after i.v. injection of ^{18}F-JNJ311

in plasma of mice and a rhesus monkey and perfused brain of mice.

MICE			
Plasma	Mean % ± standard deviation (n = 3) of intact tracer		
2 min	10 min	30 min	60 min
85 ± 3	33 ± 6	22 ± 5	11 ± 7
Perfused brain	Mean % ± standard deviation (n = 3) of intact tracer		
	10 min		60 min
	98 ± 0		94 ± 1
MONKEY			
Plasma	% (n = 1) of intact tracer		
	10 min	30 min	60 min
	51	35	28

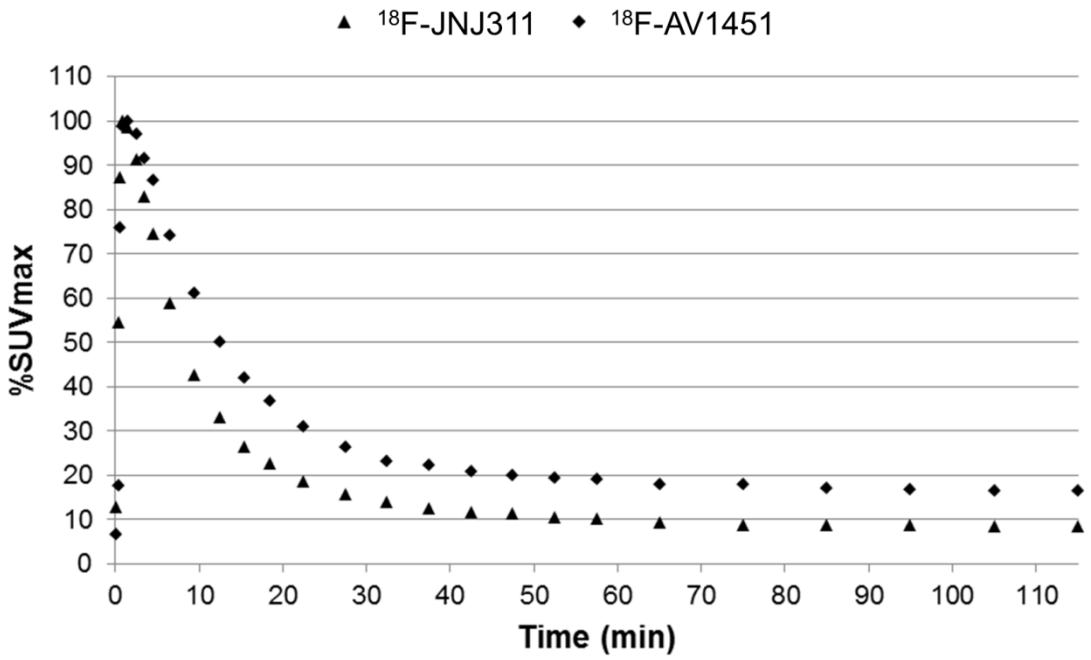

Supplemental Figure 4. $\%SUV_{max}$ curves of small animal µPET time-activity curves of ^{18}F-JNJ311 and ^{18}F-AV1451 in the whole brain of a Wistar rat.

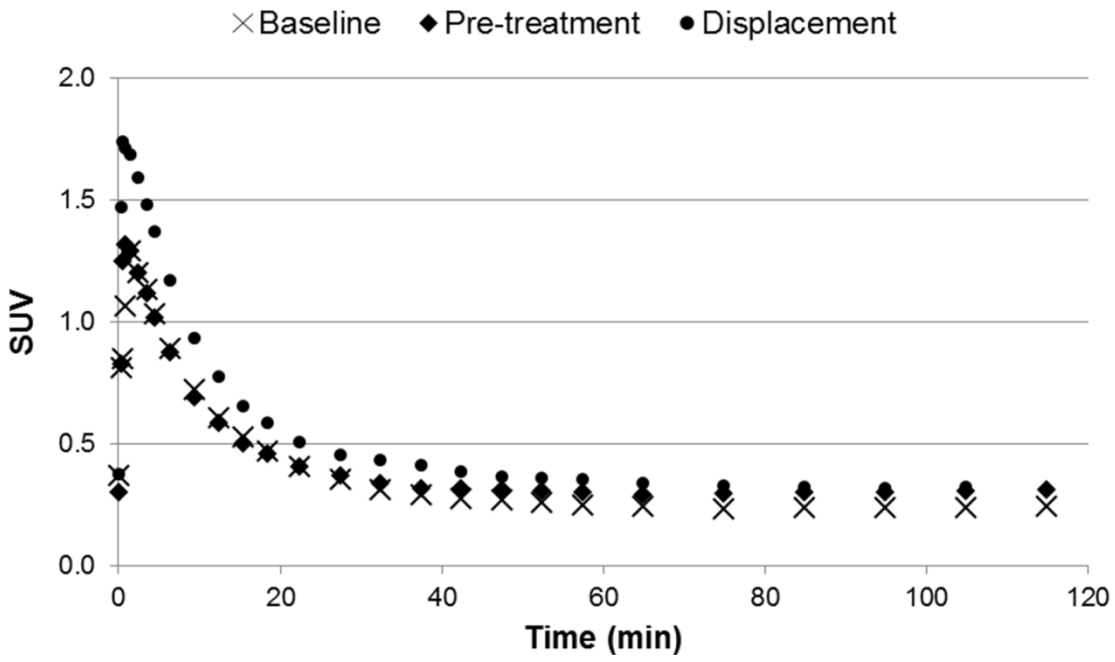

Supplemental Figure 5. Whole brain µPET time-activity curves for ^{18}F-AV1451 of three female Wistar rats. Baseline scan (n = 1); pre-treatment experiment (n = 1): pure vehicle, 10 mg/kg injected subcutaneously 60 min prior to radiotracer injection and displacement study (n = 1): pure vehicle, 1 mg/kg injected intravenously 30 min after radiotracer injection.

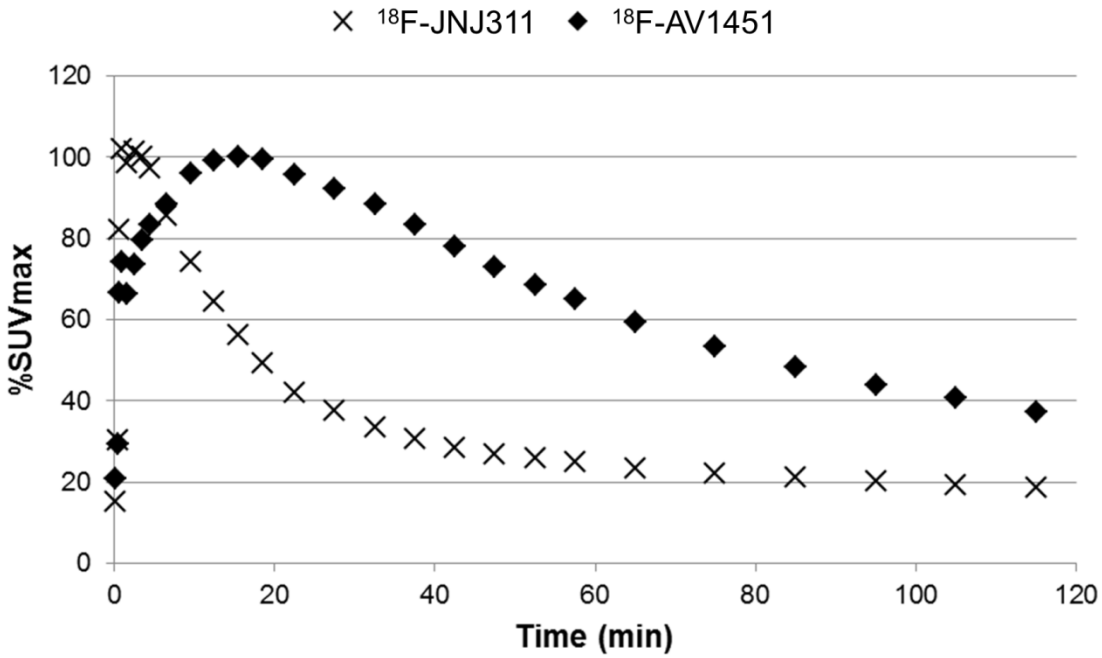

Supplemental Figure 6. Average whole brain $\%SUV_{max}$ curves of ^{18}F-JNJ311 and ^{18}F-AV1451 in a male rhesus monkey.